HHS Public Access

Author manuscript

Dalton Trans. Author manuscript; available in PMC 2016 June 28.

Published in final edited form as:

Dalton Trans. 2015 June 28; 44(24): 11067–11076. doi:10.1039/c5dt01614b.

Design, Synthesis and Characterisation of New Chimeric Ruthenium(II)-Gold(I) Complexes as Improved Cytotoxic Agents

Lara Massai[‡,a,b], **Jacob Fernández-Gallardo**[‡,b], **Annalisa Guerri**[a], **Annarosa Arcangeli**[c], **Serena Pillozzi**[c], **María Contel**[b,d], and **Luigi Messori**[a]

[a]Laboratory of Metals in Medicine, Department of Chemistry, University of Florence, via della Lastruccia 3, 50019 Sesto Fiorentino, Florence, Italy. luigi.messori@unifi.it Ph: (+39) 055-457-3388 Fax: (+39) 055-457-3385.

[b]Department of Chemistry, Brooklyn College - The City University of New York, Brooklyn, NY, 11210, US. mariacontel@brooklyn.cuny.edu., Ph: (+1) 7189515000 x2833 Fax: (+1) 7189514607.

[c]Department of Experimental and Clinical Medicine, University of Florence, Viale GB Morgagni 50, 50134 Firenze, Italy.

[d]Chemistry and Biology PhD Programs, The Graduate Center, The City University of New York, 365 Fifth Avenue, New York, NY 10016, US.

Abstract

Two heterobimetallic complexes, *i.e.* [$RuCl_2$(p-cymene)(μ-dppm)AuC] (**1**) and [$RuCl_2$(p-cymene)(μ-dppm)Au S(thiazoline)] (**3**), based on known cytotoxic [Ru(p-cymene)$Cl_2(PR_3)$] and [$AuX(PR_3)$] (X = Cl, SR) molecular scaffolds, with the diphosphane linker 1,1-bis(diphenylphosphino) methane, dppm, were conveniently prepared and characterised. Remarkably, the new compounds manifested a more favourable *in vitro* pharmacological profile toward cancer cells than individual ruthenium and gold species being either more cytotoxic or more selective. The interactions of the study compounds with (pBR322) DNA and their inhibitory effects on cathepsin B were also assessed. In addition, their reactivity toward suitable models of protein targets was explored and clear evidence gained for disruption of the bimetallic motif and for protein binding of monometallic fragments. Overall, the data reported here strongly support the concept of multifunctional heterometallic compounds as “improved” candidate agents for cancer treatment. The mechanistic and pharmacological implications of the present findings are discussed.

Introduction

Metal based drugs play a crucial role in current treatment protocols of cancer owing to the large clinical success of platinum based agents. However, as established platinum drugs show a number of serious drawbacks such as a relatively limited spectrum of anticancer

Correspondence to: María Contel; Luigi Messori.

‡These authors contributed equally to this work.

†Electronic Supplementary Information (ESI) available: [crystallographic information for compound 1, UV-VIS and ESI/MS spectra overtime, detailed cytotoxicity studies, NMR spectra over time, selected IR spectra].

activities, severe systemic toxicity and frequent insurgence of chemo-resistance, intense research efforts are currently being made to discover new anticancer metallodrugs with distinct and more favourable anticancer profiles.

The rich coordination chemistry of transition metals offers a multitude of opportunities to synthesize innovative compounds by rational design that may turn highly suitable for cancer treatment. Thus, beyond the clinically established platinum complexes, much attention has been paid to other classes of medicinal metallodrugs containing various metal centers such as copper, ruthenium, gold, titanium, etc.

In particular, ruthenium compounds triggered a lot of interest within the "*Metals in Medicine*" scientific community, during the last two decades, with a few compounds that already entered clinical trials or have undergone advanced pre-clinical testing. The majority of these ruthenium compounds were reported to display moderate to relevant antitumor and/or antimetastatic activities accompanied by a relatively low systemic toxicity *in vivo*.[1–8]

Another promising family of metallodrugs for cancer chemotherapy is that of gold complexes. Indeed, a number of cytotoxic gold compounds were found to overcome cisplatin resistance in specific cancer cells[9–11] which makes them attractive potential therapeutics. In general, gold compounds manifest a high degree of cell toxicity; yet, the precise mechanisms of antitumor activity of gold compounds are not understood. A number of mechanistic studies revealed that gold binding to the selenoenzyme thioredoxin reductase (TrxR)[12,13] causes its strong inhibition, which results in the alteration of mitochondrial functions, increased formation of reactive oxygen species and eventual cell death *via apoptosis*.

In addition, it was shown that DNA is not the primary target for most gold compounds[14,15] reinforcing the idea that their mode of action is profoundly different from that of platinum drugs.

A recent strategy in the field of metal based anticancer drugs consists in the design of bimetallic or even multimetallic agents bearing diverse metal centers with distinct biological and pharmacological features.[16,17] This strategy is aimed to exploit the possible synergism existing among the individual metal centers, which may contribute to overcome resistance. The underlying rationale is that the incorporation of two or more metals with different biological and cytotoxic profiles within the same molecule, may greatly modify and/or improve the antitumor properties of the resulting species. This is likely due to two main factors: *a*) the interactions of the different metal centers with multiple and distinct biological targets may lead to a net synergism; b) improved physico-chemical and bio-distribution properties may characterise the bimetallic species with respect to the respective monometallic fragments.

There are a few relevant examples for this kind of strategy in the recent literature including examples reported by some of us. Bimetallic or trimetallic molecules such as titanocenes incorporating Ru(II), Pt(II) and Pd(II) centers,[18,19] and a number of derivatives containing ferrocene moieties and other metals[20] were recently described. Heterometallic compounds incorporating gold(I) fragments have been reported for titanocene,[19,21,22] ruthenocene,[23]

platinum(II)[24] and rhenium(I) derivatives.[25] Ferrocenyl phosphanes were also incorporated in the iminophosphorane skeleton of gold(III) coordination complexes.[20]

In general, a significant improvement of the cytotoxic properties for heterometallic complexes in comparison with the mixture of the two monometallic precursors may be expected and is often documented. In addition, the incorporation of gold and of a second metal within the same molecule may offer advantages in their use as potential anticancer derivatives. Improved stability,[21–22] solubility[21,22] or lower toxicity *in vivo*[22] with respect to the individual monometallic fragments, or a beneficial combination of medicinal properties (*e.g.* a cell imaging agent *plus* a cytotoxic agent)[22] were reported. Nevertheless, studies on the possible mechanism of heterometallic complexes are still scarce[19,20,22] and at a preliminary stage, and there is definitely a real need to understand their interactions with different biological targets to assess the role exerted by each individual metal center.

Within this frame, we found the idea of combining two of the most promising metallic fragments i.e. a ruthenium(II)-*p*-cymene-phosphane derivative (with potential cytotoxic/antimetastatic properties) and a gold(I)-phosphane-chloride or -thiolate fragment (with well-known cytotoxic properties) a feasible working hypothesis to obtain novel chimeric chemotherapeutics with improved properties. Specifically, we report here on the preparation, characterization and stability of two such bimetallic Ru(II)-Au(I) complexes. The new compounds are depicted in Chart 1. They contain a ruthenium(II) *p*-cymene dichloride fragment and a gold(I) chloride (**1**) or thiolate (**3**) fragment linked through a bifunctional diphosphane ligand 1,1-bis (diphenylphosphino) methane (dppm).

The antiproliferative properties of **1** and **3** were assessed toward a representative cancer cell line as well as a non-cancerous cell line and compared to those of control ruthenium and gold monometallic species. We also report here some preliminary studies of their interactions with a few typical biomolecular targets (DNA, cathepsin B and model proteins) to gain further mechanistic information. Importantly, this is the first time that interactions of heterometallic compounds with proteins are described taking advantage of ESI/MS spectrometric techniques.

Results and Discussion

Chemistry

Synthesis and characterisation of the two Ru-Au heterodimetallic complexes

—The synthetic procedure is described in Scheme 1. The ruthenium dimer [Ru(*p*-cymene)Cl(μ-Cl)]$_2$[26] was reacted in a 1:1 ratio with [AuCl(μ-dppm)]$_2$[27] to give compound **1** in high yield. The synthesis of the thiolate analogue (**3**) was successfully achieved by addition of the Ru(II) derivative containing dppm [Ru(*p*-cymene)Cl$_2$(η^1-dppm)][28,29] to the polymeric insoluble material [Au(S-thiazoline)]n (**2**).

Compounds **1** and **3** were characterized unambiguously by $^{31}P\{^1H\}$, ^1H and $^{13}C\{^1H\}$ NMR and IR spectroscopy and by elemental analysis (see experimental section and SI).
The $^{31}P\{^1H\}$ NMR spectra in $CDCl_3$ of **1** and **3** show two distinct doublets at 21.64/17.80

ppm (**1**) and 22.62/21.22 ppm (**3**) due to coordination of the dppm ligand to the Au(I) and Ru(II) centers respectively.

Crystal structure determination for complex 1—The solid-state structure for compound **1** was determined by single-crystal X-ray diffraction. The structure is shown in Figure 1 and selected bond distances (Å) and angles (°) are compiled in Table 1. The asymmetric unit of the structure of **1** contains one molecule of the complex and one molecule of the solvent dichloromethane in which crystals of **1** were obtained. All the atoms of the solvent molecule have an occupancy factor of 0.5. Coordination bond lengths and angles of the two metal ions are reported in Table S1 (See Supporting Information) and are in agreement with those found for similar complexes retrieved in a search in the CSD (v. 1.16).[30] The gold(I) metal atom has the usual almost linear coordination. The bond lengths Au(1)-P(2) and Au(1)-Cl(3) are respectively 2.228(2) and 2.275(4) Å while the angle P(2)-Au(1)-Cl(3) is 177.88(9)°. The ruthenium(II) ion exhibits the expected pseudo octahedral three legged piano-stool arrangement common for half-sandwich Ru(II) phosphine complexes.[31] The angles between P(1), Cl(1) and Cl(2) of the three legs, the ruthenium atom and the centroid of the aromatic ring of the cymene moiety are respectively 131.51, 126.48 and 124.95°, as found commonly for this geometry. The aromatic rings C(17)-C(22) and C(30)-C(35) interact *via* a π stacking intramolecular interaction, being the distance between the centroids of the two planes 3.75 Å and the angles between the mean planes 173.44(7)°.

In the unit cell, a π stacking interaction is also observed involving the same aromatic rings C(24)-C(29) of two different molecules, one of these obtained by the symmetry operation −x +2, −y, −z+2. The distance of the centroid of the two rings is 4.714 Å. The hydrogen atom H(27) of the same residue interacts with the chlorine atoms Cl(1) and Cl(2) of the same molecule (i.e. reported by the s.o. −x+2, −y, −z+2) being the distance 2.918(3) and 2.979(2) Å respectively and the angles 126.9(2) and 162.1(1)°.

Stability in solution through UV-vis, ^{1}H and ^{31}P{^{1}H} NMR spectroscopy analysis—The solution behaviour of these heterodimetallic complexes was analysed to assess their suitability for biological studies. First, the stability in DMSO-d_6 of **1** and **3** was studied by NMR spectroscopy. The compounds are soluble in mixtures 1:99 DMSO/H_2O or buffer at micromolar range but the concentrations needed for NMR spectroscopy are larger and neat DMSO-d_6 was used in these studies. It was found that the compounds have a half-life of at least 48 hours (see Figures S18–S21 in SI). Next, the stability of **1** and **3** in ammonium acetate buffer (containing 0.3% DMSO) was examined by UV-vis spectroscopy. A small amount of concentrated solutions of the individual complexes was freshly prepared in DMSO. The electronic spectra were recorded directly in DMSO and in the reference buffer at a final concentration of 30 μM. From spectra inspection it is apparent that the various compounds manifest a substantial stability with no evidence of major changes even over an observation period of three days (72h). This is indeed a sufficiently long period to reach their biological target. Yet, some minor spectral alterations were noticed in the spectra of compound **1** that may be ascribed to partial detachment of the weak ligands (chloride) from the metal coordination sphere. To confirm this hypothesis, complete detachment of the chlorido ligand was achieved by addition of excess $AgNO_3$; results indicate that the

exchange of ligand leads to appreciable spectral variations (See Supporting Information Figures S1–S3). Moreover, from spectral analysis, it is apparent that protein addition does not affect the metal chromophore in a significant way. In turn, the spectra of the various metallodrug-cyt c systems reveal that the protein chromophore is substantially stable over 24 hours, with cyt c remaining in its oxidised ferric form (See Figure S4 in SI).

Cellular studies

The antiproliferative properties of the heterobimetallic complexes **1** and **3** and those of ruthenium and gold complexes chosen as reference (Chart 2) were subsequently assayed by monitoring their ability to inhibit cell growth using the Trypan Blue Assay(see Experimental Section). The cytotoxic activity of the various compounds was first determined toward the human cancer cell HCT116 (colon carcinoma) as described in the Experimental Section. Afterward, to assess selectivity towards cancer cells their effects on a non-carcinogenic mouse fibroblast cancer cell line L929 were also evaluated. Results are summarized in Table 2.

Compound $[Au(S\text{-thiazoline})]_n$ (**2**) is a polymer insoluble in most organic solvents and DMSO and for this reason was not evaluated.

A dose-dependent inhibition of cell growth was observed in HCT116 cell lines with IC50 values ranging in the micromolar scale, as depicted in Figure 2 and S6, for all tested compounds.

The heterobimetallic compounds **1** and **3** are far more cytotoxic than both ruthenium compounds *i.e.* dimer $[Ru(p\text{-cymene})Cl(\mu\text{-}Cl)]_2$ (**a**) and $[Ru(p\text{-cymene})Cl_2(\eta^1\text{-dppm})]$ (**b**). Moreover, as shown in Table 2, the IC90 values, for both compounds (**a** and **b**) are ~ 100 times greater than the respective IC50 values. Those complexes manifest a strong dose-dependence, indicating that, to enhance efficacy toward cancer cells, a remarkably increased dose is needed. Additionally, we confirmed the elevated cytotoxicity of the starting material $[AuCl(\mu\text{-dppm})]_2$ (**c**).

It is important to remind that various gold(I) compounds with phosphane ligands were discarded in the past as potential anticancer agents due to their elevated toxicity *in vivo* greatly affecting essential healthy organs.[22] This implies that particular attention must be paid to the selectivity issue. Remarkably, the values reported in Table 2 highlight that both heterobimetallic compounds manifest a greatly improved selectivity for cancer cells when compared to the cytotoxic $[AuCl(\mu\text{-dppm})]_2$ (**c**).

Compound $[Ru(p\text{-cymene})Cl_2(\eta^1\text{-dppm})]$ (**b**) had been described as having a high cytotoxicity while possessing selectivity towards cancer cell lines.[32] We tested its cytotoxicity in the cancer cell line HCT116 and demonstrated that heterobimetallic compounds **1** and **3** had also a lower IC_{50} than this compound for this cell line.

The activities of the tested compounds against normal cells are shown in Table 2. Normal cells tunred out to be far less sensitive to these experimental compounds than cancer cells.

Tumour selectivity data are shown in Table 3. Tumour selectivity is calculated as the IC50 values for primary cultures divided by the IC50 values for the cancer cells.

Compounds **1** and **3** exhibited a greater selectivity towards tumour cells and were consequently less toxic to t normal cells. Heterobimetallic complexes were more selective towards cancer cells than normal cells by a factor of ~ 7.5

Overall, these results support the concept that Ru-Au dimetallic complexes are more effective than the parent ruthenium(II) species in terms of cytotoxic potential and selectivity. Additionally, they show a far greater selectivity for cancer cells than the gold(I) phosphane reference compound.

Biomolecular Interactions

To gain a more comprehensive insight of the chemical and biological profile of heterometallic compounds **1** and **3** we studied their interactions with a few relevant biomolecules by various biophysical techniques. Results of these studies are described below.

Interactions with DNA

First, we analyzed the interactions of **1** and **3** with representative DNA molecules. Specifically, we carried out gel electrophoresis studies to disclose the effects of the new heterobimetallic compounds and of the reference dinuclear Ru and Au complexes on plasmid (pBR322) DNA (Figure 3). The interactions of [Ru(*p*-cymene)Cl_2(η^1-dppm)] with DNA by different techniques (including gel electrophoresis) had previously been reported.[32]

Plasmid (pBR322) DNA presents two main forms: OC (open circular or relaxed form, Form II) and CCC (covalently closed or supercoiled form, Form I). Changes in electrophoretic mobility of both forms are usually taken as an evidence of metal-DNA binding. Generally, the larger the retardation of supercoiled DNA (CCC, Form I), the greater the DNA unwinding produced by the drug.[33] Treatment with increasing amounts of Ru(II), Au(I) compounds **a** and **c** or heterometallic RuAu derivatives **1** and **3** did not affect the mobility of the faster-running supercoiled form (Form I) even at the highest molar ratios (d). Compound [Ru(*p*-cymene)Cl_2(η^1-dppm)] weakly reduced supercoiling in plasmid DNA and, in general, its effect on unwinding DNA was smaller compared to other Ru(II) arene phosphine derivatives. However, it was shown that this complex was able to bind DNA in a non-intercalative fashion.[33] The lack of interaction between the heterobimetallic compounds and plasmid (pBR322) DNA (already observed for other Ru(II)-arene derivatives[4–8] and Au(I) derivatives[22]) points out that other biomolecular targets are probably implicated in the cell death pathways.

Inhibition of cathepsin B

Cathepsin B (cat B) is an abundant and ubiquitously expressed cysteine peptidase of the papain family, which has turned out to be a reliable prognostic marker for several types of cancers.[34] Cathepsin B seems to be involved (along with other cathepsins) in metastasis, angiogenesis, and tumor progression.[35] Cat B has been proposed as a possible therapeutic

target for the control of tumor progression.[36] Indeed, RAPTA Ru compounds which inhibit cat B with IC50 values in the low micromolar range effectively reduce the mass and the number of metastases *in vivo*.[37] We therefore, studied the inhibition of Cat B by compounds **1, 3** and by ruthenium [Ru(*p*-cymene)Cl_2(η^1-dppm)] (see experimental section for details and IC50 values in Table 3). All three compounds turned out to inhibit Cat B. The IC50 for compounds [Ru(*p*-cymene)Cl_2(η^1-dppm)] and **3** were 143 and 190 μM respectively. Compound **1** containing the gold-chloride fragment resulted far more active with an IC50 value of 31 μM. It was previously reported that compound [Ru(*p*-cymene)Cl_2(η^1-dppm)] displays not only cytotoxic but also strong antimetastatic properties as it prevented cell invasion through matrigel.[32] It was hypothesized that a correlation between inhibition of Cat B and inhibition of metastasis does exist. Compound **1** inhibits Cat B ca. 4.6 times more efficiently than [Ru(*p*-cymene)Cl_2(η^1-dppm)]. These results are encouraging and suggest to test the metastasis inhibitory properties of compound **1** or of some analogues in the future.

Compound **3** containing the thiol group displays a lower IC50 than compound **1** and in the same order than [Ru(*p*-cymene)Cl_2(η^1-dppm)]. However, it is known that gold(I)-thiolate moieties also containing phosphanes are cytotoxic and that their cell death effects are due at least in part, to the inhibition of thioredoxin reductase.[38] This may be the case for the heterobimetallic Ru-Au compound **3** as well. In general gold-thiolate-phosphane complexes result also toxic to normal cell lines and we have demonstrated how the incorporation of the ruthenium(*p*-cymene) fragment seems to improve the selectivity for cancer cells of bimetallic Ru-Au molecules.

ESI-MS studies : model proteins/complexes interactions

We further analysed the reactions of the two heterobimetallic complexes **1** and **3** and those of the reference dinuclear ruthenium(II) complexes [(*p*-cymene)RuCl(μ-Cl)]$_2$ (**a**) and [Ru(*p*-cymene)Cl_2(η^1-dppm)] (**b**) with model proteins to gain a deeper mechanistic insight into their likely interaction mode with biomolecular targets. Metallodrug-protein interactions with the model proteins were analysed through ESI MS analysis according to established experimental protocols developed in our laboratory.[39] ESI-MS spectra, recorded on the various samples at the end of the incubation period, turned out particularly informative in revealing adduct formation and in determining the final metal to protein stoichiometry and the nature of protein bound metallic fragments. Representative ESI-MS spectra are shown in Figure 4. The number and the nature of protein bound metallic species could be determined unambiguously. A rough estimate of the amount of protein metalation was achieved by comparing the experimental peak intensities-*i.e.* the peak of the free protein versus those of its metal adducts. Thus, ESI-MS analysis allows for a quite detailed interpretation of the binding process in the different cases. Notably, we observed partial or, in some cases, even total fragmentation of the heterometallic compounds.

Both compounds, **1** and **3**, showed high affinity towards cytochrome c. For both compounds, the protein bound molecular fragment was the same, i.e. the Ru(*p*-cymene) moiety. For compound **3**, an extra peak that could be assigned to a naked gold(I) fragment bound to the protein was clearly detected. Remarkably, **1** manifested a very high reactivity towards RNase accompanied by the formation of relatively large amounts of adducts bearing the Ru(*p*-

cymene) moiety. In addition for RNase, other peaks can be assigned to new protein-metal adducts such as those arising from protein binding of one or two “naked” gold(I) ions and of a “naked” ruthenium(II) ion. In the case of HEWL, only small amounts of metal-protein adducts were identified.

Overall, we could ascertain that the three tested compounds behave as classical prodrugs; indeed, upon “chemical activation”, consisting in the removal of at least one weak ligand, they react with model proteins either upon partial disruption of the starting complex or through total complex disruption. In the latter case, the bare metal ion acts as the protein reactive species and binds to them in a covalent fashion. In any case, some significant differences were highlighted in the relative efficiency of the various metalation processes and in the quantities of the adducts formed.

All three proteins manifest a higher affinity towards ruthenium than gold ions. This is in agreement with results obtained for reference complex [Ru(*p*-cymene)Cl(μ-Cl]$_2$ (**a**) for which the position of the main peak for metal-protein adducts, especially with RNase and cytc, is consistent with protein binding of a Ru(*p*-cymene) fragment with different stoichiometries (Figure S5, Supporting Information). Conversely, the dinuclear reference gold compound [AuCl(μ-dppm)]$_2$ (**c**) did not interact with any model proteins (data not shown).

On the whole, these results indicate that proteins, rather than DNA, are preferetnail biomolecular targets for our complexes. Compound **1** and **3** react differently with model proteins and with cathepsin B; such differences in reactivity can lead to select different biomolecular targets or pathways inside the cells.

Experimental

Synthesis

General—[AuCl(tht)],[40] [Ru(*p*-cymene)Cl(μCl)]$_2$[26] were prepared as previously reported. [AuCl(μ-dppm)]$_2$[27] and [Ru(*p*-cymene)Cl$_2$(η^1-dppm)][28,29] were prepared by modification of the reported synthetic strategies. Bis(diphenylphosphino)-methane (dppm) and 2-mercaptothiazoline (HS-thiazoline) were purchased from Sigma Aldrich and used without further purification. NMR spectra were recorded in a Bruker AV400 (^{1}H NMR at 400 MHz, ^{13}C NMR at 100.6 MHz and ^{31}P NMR at 161.9 MHz. Chemical shifts (δ) are given in ppm using $CDCl_3$ as the solvent, unless otherwise stated. ^{1}H and ^{13}C NMR resonances were measured relative to solvent peaks considering tetramethylsilane = 0 ppm, and ^{31}P{^{1}H} NMR was externally referenced to H_3PO_4 (85%). Coupling constants J are given in hertz. IR spectra (4000250 cm^{-1}) were recorded on a Nicolet 6700 Fourier transform infrared spectrophotometer on Nujol mulls. Elemental analyses were performed on a Perkin-Elmer 2400 CHNS/O series II analyzer.

[AuCl(μ-dppm)]$_2$—[AuCl(tht)] (0.184 g, 0.57 mmol) and dppm were dissolved in dichloromethane (15 mL) giving rise to a colorless solution that was stirred at RT for 15 minutes. Afterwards, the solvent volume was reduced to ~3 mL. Addition of 20 mL of *n*-hexane led to the formation of a white solid that was filtered off and washed with *n*-hexane

(3 × 10 mL) and diethyl ether (3 × 10 mL). $[AuCl(dppm)]_2$ was then isolated as a white powder in 96% yield (0.341 g). The ^1H and $^{31}P\{^1H\}$ NMR in DMSO-d_6 data match those previously reported.[27]

[Ru(*p*-cymene)Cl_2(η^1-dppm)]—A colorless solution of dppm (0.208 g, 0.57 mmol) in 10 mL of dichloromethane (0.054 M) was dropwise added to a brown solution of [Ru(*p*-cymene)Cl(μ-Cl)]$_2$ (0.166 g, 0.27 mmol) in 10 mL of dichloromethane (0.027 M). This addition underwent a red-brown turbid solution that became clear and bright red after being stirred at RT for 5 hours. Solvent removal under reduced pressure gave rise to an red solid that was washed with cold diethyl ether (0 °C, 3 × 5 mL) to yield the final product in 92% yield (0.345 g). ^1H and $^{31}P\{^1H\}$ NMR data matched those previously reported.[26]

[Ru(*p*-cymene)Cl_2(μ-dppm)AuCl] (1)—[Ru(*p*-cymene)Cl(μ-Cl)]$_2$ (0.061 g, 0.10 mmol) and [AuCl(μ-dppm)]$_2$ (0.123 g, 0.10 mmol) were dissolved in dichloromethane (10 mL) to yield a dark-red solution that was stirred at RT for 3 hours. Dichloromethane was then removed under reduced pressure to yield an oily red solid that was washed with cold diethyl ether (0 °C, 3 × 10 mL). The red solid obtained was then recrystallized in dichloromethane by slow evaporation at RT leading to the formation of red crystals suitable for X-Ray diffraction (0.146 g, 83% yield). Anal. Calc. for $C_{35}H_{36}AuCl_3P_2Ru$ (923.01): C, 45.55; H, 3.93. Found: C, 45.61; H, 3.60. $^{31}P\{^1H\}$ NMR ($CDCl_3$): δ 21.64 (d, $^2J_{PP}$ = 21.0 Hz, Au-PPh_2), δ 17.80 (d, $^2J_{PP}$ = 25.2 Hz, Ru-PPh_2). ^1H NMR ($CDCl_3$): δ 8.11 (4H, m, PPh_2), δ 7.38-7.23 (16H, m, PPh_2), δ 5.30 (2H, d, $^3J_{HH}$ = 6.0 Hz, 3-C_6H_4), δ 5.17 (2H, d, $^3J_{HH}$ = 5.9 Hz, 2-C_6H_4), δ 4.10 (2H, dd, PCH_2P), δ 2.51 (1H, m, C*H*$(CH_3)_2$), δ 1.83 (3H, m, CH_3), δ 0.83 (6H, d, $^3J_{HH}$ = 6.9 Hz, CH(C*H*$_3)_2$). $^{13}C\{^1H\}$ NMR ($CDCl_3$, plus HSQC): δ 133.42 (d, $^2J_{PC}$ = 9.1 Hz, *o*-PPh_2), δ 132.89 (d, $^2J_{PC}$ = 14.2 Hz, *o*-PPh_2), δ 131.85 (d, $^4J_{PC}$ = 2.5 Hz, *p*-PPh_2), δ 131.32 (d, $^4J_{PC}$ = 2.5 Hz, *p*-PPh_2), 129.65 (dd, $^1J_{PC}$ = 53.1 Hz, $^3J_{PC}$ = 2.2 Hz, *ipso*-PPh_2), 129.57 (d, $^1J_{PC}$ = 53.2 Hz, $^3J_{PC}$ = 2.2 Hz, *ipso*-PPh_2), δ 128.92 (d, $^2J_{PC}$ = 12.0 Hz, *m*-PPh_2), δ 128.83 (d, $^2J_{PC}$ = 9.9 Hz, *m*-PPh_2), δ 108.65 (s, 4-C_6H_4), δ 94.38 (s, 1-C_6H_4), δ 90.45 (d, $^2J_{PC}$ = 4.5 Hz, 3-C_6H_4), δ 85.68 (d, $^2J_{PC}$ = 6.1 Hz, 2-C_6H_4), δ 30.06 (s, *C*H$(CH_3)_2$), δ 21.25 (s, CH(*C*H$_3)_2$), δ 19.50 (dd, $^1J_{PC}$ = 28.9 Hz, $^1J_{PC}$ = 19.9 Hz, CH_2), δ 17.29 (s, CH_3).

[Au(S-thiazoline)]$_n$ (2)—NaOH (0.321 g, 7.80 mmol) was dissolved in ethanol (15.6 mL, 0.5 M) under strong stirring at RT along 1 hour. 2-mercaptothiazoline (0.186 g, 1.56 mmol) was then poured into the basic solution in order to be deprotonaed. After 15 minutes, a colorless solution of [AuCl(tht)] (0.500 g, 1.56 mmol) in dichloromethane (10 mL) was added over the colorless ethanolic solution giving rise to an abundant bright pale-green precipitate. The resulting reaction mixture was stirred at RT for 3 hours yielding a white (slightly greenish) suspension that was filtered off and the isolated solid washed with deionized water (5 × 5 mL), ethanol (3 × 5 mL), dichloromethane (3 × 5 mL) and diethyl ether (3 × 10 mL). After drying *in vacuo* for 2 hours, complex **2** was isolated as a greenish white solid in 96% yield (0.473 g). Complex **2** turned out to be insoluble in all common solvents, i.e., chloroform, dichloromethane, DMSO, methanol, ethanol, diethyl ether, *n*-hexane, toluene, benzene, tetrahydrofurane. Anal. Calc. for $C_3H_4AuNS_2$ (316.15): C, 11.43;

H, 1.28; N, 4.44; S, 20.35. Found: C, 11.55; H, 1.32; N, 4.39; S, 20.41. IR (cm^{-1}): 1520 vs, 1460 s, 1377 m, 1303m, 1197 w, 1051 s, 983 m, 863 w, 268 w (Au-S).

[Ru(*p*-cymene)Cl_2(μ-dppm)Au(S-thiazoline)] (3)—Ru(*p*-cymene)Cl_2(η^1-dppm)] (0.195 g, 0.28 mmol) and [Au(S-thiazoline)]$_n$ (0.088 g, 0.28 mmol) were dissolved in dichloromethane (20 mL) giving rise to a cloudy red solution that was stirred at RT. The reaction is finished when the cloudiness is gone, i.e., after 30 minutes under strong stirring. Removal of the solvent under reduced pressure yielded an oily orange-red residue that was washed with cold diethyl ether (0 °C, 3 × 10 mL). After drying *in vacuo* for 2 hours, complex **3** was then isolated as a powdery orange-red solid in 71 % yield (0.201 g). Anal. Calc. for $C_{38}H_{40}AuCl_2NP_2RuS_2$ (1,005.75): C, 45.38; H, 4.01; N, 1.39; S, 6.38. Found: C, 45.77; H, 3.92; N, 1.32; S, 6.28. $^{31}P\{^1H\}$ NMR ($CDCl_3$): δ 22.62 (d, $^2J_{PP}$ = 23.1 Hz, Au-PPh_2), δ 21.22 (d, $^2J_{PP}$ = 22.9 Hz, Ru-PPh_2). ^1H NMR ($CDCl_3$): δ 8.12 (4H, m, PPh_2), δ 7.48-7.21 (16H, m, PPh_2), δ 5.30 (2H, d, $^3J_{HH}$ = 5.0 Hz, 3-C_6H_4), δ 5.17 (2H, d, $^3J_{HH}$ = 6.1 Hz, 2-C_6H_4), δ 4.28 (2H, dd, $^3J_{HH}$ = 8.0 Hz, N-CH_2), δ 4.10 (2H, dd, PCH_2P), δ 3.38 (2H, dd, $^3J_{HH}$ = 8.0 Hz, S-CH_2), δ 2.50 (1H, m, C*H*$(CH_3)_2$), δ 1.83 (3H, m, CH_3), δ 0.84 (6H, d, $^3J_{HH}$ = 6.9 Hz, CH(C*H*$_3)_2$). $^{13}C\{^1H\}$ NMR ($CDCl_3$, plus HSQC, plus ATP):), δ 169.79 (s, *ipso*-S-thiazoline), δ 133.47 (d, $^2J_{PC}$ = 9.0 Hz, *o*-PPh_2), δ 132.94 (d, $^2J_{PC}$ = 14.2 Hz, *o*-PPh_2), δ 131.78 (d, $^4J_{PC}$ = 2.2 Hz, *p*-PPh_2), δ 131.08 (d, $^4J_{PC}$ = 1.9 Hz, *p*-PPh_2), 130.20 (dd, $^1J_{PC}$ = 55.0 Hz, $^3J_{PC}$ = 2.5 Hz, *ipso*-PPh_2), 129.86 (d, $^1J_{PC}$ = 44.9 Hz, $^3J_{PC}$ = 2.2 Hz, *ipso*-PPh_2), δ 128.89 (d, $^2J_{PC}$ = 11.7 Hz, *m*-PPh_2), δ 128.82 (d, $^2J_{PC}$ = 9.9 Hz, *m*-PPh_2), δ 108.59 (s, 4-C_6H_4), δ 94.54 (s, 1-C_6H_4), δ 90.35 (d, $^2J_{PC}$ = 4.4 Hz, 3-C_6H_4), δ 85.71 (d, $^2J_{PC}$ = 5.9 Hz, 2-C_6H_4), δ 65.86 (s, N-CH_2), δ 37.78 (s, S-CH_2), δ 30.05 (s, *C*H$(CH_3)_2$), δ 21.29 (s, CH(*C*H$_3)_2$), δ 19.91 50 (dd, $^1J_{PC}$ = 24.0 Hz, $^1J_{PC}$ = 21.2 Hz, CH_2), 17.29 (s, CH_3).

X-ray Crystallography

Single crystals of **1** (orange prisms) were mounted on a glass fiber in a random orientation. X-ray data collection was performed on an Oxford Diffraction XCalibur Diffractometer with CCD area detector and equipped with Mo K_α radiation (λ = 0.7107 Å). Data was collected and reduced with the program CrysAlis (CCD and RED).[41] Absorption correction was applied through the program SCALE3 ABSPACK implemented in the CrysAlis suite. The structure was determined by the program SIR97[42] and refined against F^2 by full-matrix least-squares techniques using SHELXL-2013[43] with anisotropic displacement parameters for all non-hydrogen atoms. All hydrogen atoms in **1** were introduced in calculated positions and refined according to a riding model with isotropic thermal parameters. All calculations were performed by using the program PARST[44] and molecular plots were produced with ORTEP3,[45] both implemented in the Crystal Structure crystallographic software package WINGX.[46] CCDC 1049232 contain the supplementary crystallographic data for this paper. These data can be obtained free of charge from the Cambridge Crystallographic Data Centre via http://www.ccdc.cam.ac.uk/Community/Requestastructure.

UV-vis experiments

Stability studies—The electronic spectra were recorded diluting small amounts of freshly prepared concentrated solutions of the individual complexes in DMSO in the reference buffer (20 mM ammonium acetate, pH 6.8). The concentration of each compound in the

final sample was 3×10^{-5} M. The resulting solutions were monitored by collecting the electronic spectra over 72h at room temperature.

Interactions with Proteins—Electronic spectra of the model protein (lysozyme, cytochrome c and RNase) at 10 μM were recorded after the addition of each complex at a stoichiometric ratio of 3:1 (metal-to-protein) over 24h at RT, in 20 mM ammonium acetate buffer, pH 6.8.

Cellular studies

Cell cultures—HCT116 cell line was cultured in RPMI 1640 (Euroclone; Milan, Italy) with 10% Fetal Bovine Serum (FBS) (Euroclone Defined; Euroclone; Milan, Italy). We cultured at 37°C in a humidified atmosphere in 5% CO_2 in air.

Pharmacology experiments—Cells were seeded in a 96-well flat-bottomed plate (Corning-Costar, Corning, NY, USA) at a cell density of 1×10^4 cells per well in RPMI complete medium. After 48 h, viable cells (determined by Trypan blue exclusion) were counted in triplicate using a haemocytometer. Each experimental point represents the mean of four samples carried out in three separate experiments.

Trypan blue assay—Cells viability was assessed by the Trypan blue exclusion assay. In brief, 10 μl of 0.4% trypan blue solution was added to 10 μl cell suspensions in culture medium.

The suspension was gently mixed and transferred to a haemocytometer. Viable and dead cells were identified and counted under a light microscope. Blue cells failing to exclude dyes were considered nonviable, and transparent cells were considered viable. The percentage of viable cells was calculated on the basis of the total number of cells (viable plus not viable).

The IC50 value (i.e., the dose that caused apoptosis of 50% of cells), IC75 and IC90 were calculated by fitting the data points (after 48 h of incubation) with a sigmoidal curve using Calcusyn software.

Interaction of $[Ru(p\text{-cymene})Cl(\mu\text{-}Cl)]_2$, $[AuCl(\mu\text{-dppm})]_2$, compounds 1 and 3 with plasmid (pBR322) DNA by Electrophoresis (Mobility Shift Assay)—10 μL aliquots of pBR322 plasmid DNA (20 μg/mL) in buffer (5 mM Tris/HCl, 50 mM $NaClO_4$, pH = 7.39) were incubated with different concentrations of the compounds (**1, 3**, [Ru(*p*-cymene)Cl(μ-Cl)]$_2$ (**a**) and [AuCl(μ-dppm)]$_2$) (**c**), in the range 0.25 and 4.0 metal complex:DNAbp, at 37 °C for 20 h in the dark. Samples of free DNA and cisplatin-DNA were prepared as controls. After the incubation period, the samples were loaded onto the 1 % agarose gel. The samples were separated by electrophoresis for 1.5 h at 80 V in Tris-acetate/EDTA buffer (TAE). Afterwards, the gel was stained for 30 min with a solution of GelRed Nucleic Acid stain.

Inhibition of cathepsin B—Cathepsin B, purified from human liver (Accession # P07858) and substrate Peptide sequence: Z-FR-AMC [AMC=7-amino-4-methylcoumarin] were dissolved on a buffer: 25 mM MES pH 6, 50 mM NaCl, 0.005% Brij35, 5 mM DTT

and 1% DMSO with a final concentration of 10 μM. The enzyme solution was delivered into the reaction well. 2 (1% DMSO solution) was delivered into the enzyme mixture by Acoustic technology (Echo550; nanoliter range), incubate for 10 min. at room temp. The substrate solution was delivered into the reaction well to initiate the reaction. The enzyme activity was monitored (Ex/Em = 355/460 nm) as a time-course measurement of the increase in fluorescence signal from fluorescently-labeled peptide substrate for 120 min. at room temperature. The data was analyzed data by taking slope (signal/time) of linear portion of measurement. The slope is calculated by using Excel, and curve fits are performed using Prism software.

ESI-MS experiments—Metal complex/protein adducts were prepared by mixing equivalent amounts of the three proteins (100 μM) in 20 mM ammonium acetate buffer (AmAc), pH 6.8. Then the complexes were added (3:1 metal/protein ratio) to the solution and incubated at RT for 24h. After a 20-fold dilution with water, ESI-MS spectra were recorded by direct introduction at 5 μl/min flow rate in an Orbitrap high-resolution mass spectrometer (Thermo, San Jose, CA, USA), equipped with a conventional ESI source. The working conditions were the following: spray voltage 3.1 kV, capillary voltage 45 V and capillary temperature 220°C. The sheath and the auxiliary gases were set, respectively, at 17 (arbitrary units) and 1 (arbitrary units). For acquisition, Xcalibur 2.0. software (Thermo) was used and monoisotopic and average deconvoluted masses were obtained by using the integrated Xtract tool. For spectrum acquisition a nominal resolution (at m/z 400) of 100,000 was used.

Conclusions

To summarize, we have designed two novel organometallic ruthenium(II)-gold(I) species with the goal of obtaining chimeric bifunctional molecules bearing improved chemical, biological and pharmacological properties.

The two new complexes were characterised both in the solid state and in solution. They manifest acceptable stability and solubility profiles in aqueous environments that render them well amenable for standard *in vitro* pharmacological testing.

Afterward, the antiproliferative properties of these two bimetallic complexes were assayed in comparison to the corresponding mononuclear ruthenium(II) species in a representative cancer cell line. Similar patterns of antiproliferative properties emerged for both complexes irrespective of the nature of the terminal ligand on the gold(I) center. Remarkably, both heterobimetallic complexes turned out to be considerably more active than the parent binuclear ruthenium compound [Ru(*p*-cymene)Cl(μ-Cl)]$_2$ and more active than mononuclear ruthenium derivative containing dppm [Ru(*p*-cymene)Cl$_2$(η^1-dppm)], implying that tethering of the Au center in the molecular scaffold of the ruthenium complex provides a relevant contribution to the measured biological activity. The increased cytotoxicity probably arises from the contribution of the gold(I) center owing to its high affinity for thiol/selenol residues in proteins/enzymes and its known cytotoxicity. In addition, the new bimetallic compounds turned out to be far more selective to cancer cells than the gold(I) starting material [AuCl(μ-

dppm)]$_2$ -while less cytotoxic-underscoring the beneficial effect of the coordination of a ruthenium(II)(*p*-cymene) fragment in the resulting bimetallic molecule.

From the studies of the interactions of the study compounds with plasmid (pBR322) DNA it was inferred that these heteronuclear metallodrugs probably act through a pharmacological mechanism where nucleic acids are not the only or primary targets. This was further confirmed in the case of compound **1** for which inhibition of purified cathepsin B was achieved in the micromolar range.

Finally, the reactions of these heterobimetallic compounds with model proteins were evaluated. Unambiguous evidence was gained that these dimetallic complexes eventually break down upon reaction with proteins and that ruthenium fragments are primarily found associated to proteins; however in some cases evidence of protein bound to gold ions was also obtained.

Overall, this study nicely supports the concept that it is possible to design specific heterobimetallic (chimeric) species with enhanced antiproliferative properties and more favourable anticancer profiles than individual monometallic counterparts. In perspective, several other metal combinations may be explored more systematically to optimise the synergism existing between the individual metal centers. Furthermore, through an appropriate choice of the linker and of the ancillary ligands, it may be possible to finely tune the stability of the dimetallic moiety and govern its fate within biological environments.

Supplementary Material

Refer to Web version on PubMed Central for supplementary material.

Acknowledgements

We gratefully acknowledge Beneficentia Stiftung (Vaduz, Liechtenstein), AIRC (IG-12085) and COST Action CM1105 for generous financial support. Research at Brooklyn College was supported by a grant from the National Cancer Institute (NCI) 1SC1CA182844 (M.C.). We thank Dr. Elena Michelucci for recording ESI-MS spectra

References

1. Bergamo A, Gaiddon C, Schellens JHM, Beijnen JH, Sava GG. J. Inorg. Biochem. 2012; 106:90. [PubMed: 22112845]
2. Nazarov AA, Hartinger CC, Dyson PJ. J. Organomet. Chem. 2104; 751:251.
3. Rademaker-Lakhai JM, van der Bongard D, Pluim D, Beijnen JH, Schellens JMH. Clinical Cancer Res. 2004; 10:3717. [PubMed: 15173078]
4. Hartinger CG, Zorbas-Seifried S, Jakupec MA, Kynast B, Zorbas H, Keppler BK. J. Inorg. Biochem. 2006; 10:9891.
5. Bergamo A, Masi A, Peacock AFA, Habtemariam A, Sadler PJ, Sava G. J. Inorg. Biochem. 2010; 104:79. [PubMed: 19906432]
6. Adhireksan Z, Davey GE, Campomanes P, Groessl M, Clavel CM, Yu H, Nazarov AA, Fang Yeo CH, Ang WH, Droge P, Rothlisberger U, Dyson PJ, Davey CA. Nat. Commun. 2014; 5:3462. [PubMed: 24637564]
7. Weiss A, Berdsen RH, Dubois M, Müller C, Schibli R, Griffioen AW, Dyson PJ, Nowak-Sliwinska P. Chem. Sci. 2014; 5:4742.

8. Frik M, Martinez A, Elie BT, Gonzalo O, Ramirez de Mingo D, Sanau M, Sanchez-Delgado R, Sadhukha T, Prabha S, Ramos JW, Marzo I, Contel M. J. Med. Chem. 2014; 57:9995. [PubMed: 25409416]
9. Bertrand B, Casini A. Dalton Trans. 2014; 43:4209. [PubMed: 24225667]
10. Berners-Price SJ, Filipovska A. Metallomics. 2011; 3:863. [PubMed: 21755088]
11. Sun RW-Y, Lok C-N, Fong TT-H, Li CK-L, Yang ZF, Zou T, Siu F-M, Che C-M. Chem. Sci. 2013; 4:1979.
12. Schuh E, Pflüger C, Citta A, Folda A, Rigobello MP, Bindoli A, Casini A, Mohr F. J Med Chem. 2012; 55(11):5518. [PubMed: 22621714]
13. Serebryanskaya TV, Lyakhov AS, Ivashkevich LS, Schur J, Frias C, Prokopd A, Ott I. Dalton Trans. 2015; 44:1161. [PubMed: 25413270]
14. Nobili S, Mini E, Landini I, Gabbiani C, Casini A, Messori L. Med. Res. Rev. 2010; 30:550. [PubMed: 19634148]
15. Liu W, Bensdorf K, Proetto M, Hagenbach A, Abram U, Gust R. J Med Chem. 2012; 55(8):3713. [PubMed: 22424185]
16. Schulz J, Renfrew AK, Císařová I, Dyson PJ, Štěpnička P. Appl. Organometal. Chem. 2010; 24:392.
17. Khan RA, Asim A, Kakkar R, Gupta D, Bagchi V, Arjmand F, Tabassum S. Organometal. 2013; 32:2546.
18. Pelletier F, Comte V, Massard A, Wenzel M, Toulot S, Richard P, Piquet M, Le Gendre PD, Zava O, Edafe F, Casini A, Dyson PJ. J. Med. Chem. 2010; 53:6923. [PubMed: 20822096]
19. Gonzalez-Pantoja JF, Stern M, Jarzecki AA, Royo E, Robles-Escajeda E, Varela-Ramirez A, Aguilera RJ, Contel M. Inorg. Chem. 2011; 50:11099. [PubMed: 21958150]
20. Lease N, Vasilevski V, Carreira M, de Almeida A, Sanaú M, Hirva P, Casini A, Contel María. J. Med. Chem. 2013; 56:5806. and refs. there in. [PubMed: 23786413]
21. Wenzel M, Bertrand B, Eymin MJ, Comte V, Harvey JA, Richard P, Groessel M, Zava O, Amrouche H, Le Gendre PD, Piquet M, Casini A. Inorg. Chem. 2011; 50:9472. [PubMed: 21875041]
22. Fernandez-Gallardo J, Elie BT, Sulzmaier F, Sanaú M, Ramos JW, Contel M. Organometallics. 2014; 33:6669. [PubMed: 25435644]
23. Bjelosevic H, Guzei IA, Spencer LC, Persson T, Kriel FH, Hewer R, Nell MJ, Gut J, van Resburg CEJ, Rosenthal P, Coates J, Darkwa J, Elmroth SKC. J. Organomet. Chem. 2012; 720:52.
24. Wenzel M, Bigaeva E, Richard P, Le Gendre P, Picquet M, Casini A, Bodio E. J. Inorg. Biochem. 2014; 141:10. [PubMed: 25172993]
25. Fernandez-Moreira V, Marzo I, Gimeno C. Chem. Sci. 2014; 5:4434.
26. Tönnemann J, Risse J, Grote Z, Scopelliti R, Severin K. Eur. J. Inorg. Chem. 2013; 2013:4558.
27. Schmidbaur H, Wohlleben A, Schubert U, Frank A, Huttner G. Chemische Berichte. 1977; 110:2751.
28. Daguenet C, Dyson P. Catal. Comm. 2003; 4:153157.
29. Gupta D, Sahay A, Pandey D, Jha N, Sharma P, Espinosa G, Cabrera A, Puerta M, Valerga P. J. Organometal. Chem. 1998; 568:1320.
30. Allen FH. Acta Cryst B. 2002; B58:380. [PubMed: 12037359]
31. (a) Chandrasekaran P, Mague JT, Balakrishna MS. Polyhedron. 2013; 27:80.(b) Aznar R, Grabulosa A, Mannu A, Muller G, Sainz D, Moreno V, Font-Bardia M, Calvet T, Lorenzo J. Organometallics. 2013; 32:2344–2362.
32. Das S, Sinha S, Britto R, Somasundaram K, Samuelsom AG. J. Inorg. Biochem. 2010; 104:93. [PubMed: 19913918]
33. Cutts SM, Casta A, Panousis C, Parsons PG, Sturm RA, Phillips DR. Methods Mol. Biol. 1997; 90:95. [PubMed: 9407529]
34. Koblinski JE, Ahram M, Sloane BF. Clin. Chim. Acta. 2000; 291:113. [PubMed: 10675719]
35. Joyce JA, Baruch A, Chedade K, Meyer-Morse N, Giraudo E, Tsai F-Y, Greenbaum DC, Hager JH, Bogyo M, Hanahan D. Cancer Cell. 2004; 5:443. [PubMed: 15144952]

36. Frlan R, Gobec S. Curr. Med. Chem. 2006; 13:2309. [PubMed: 16918357]
37. Casini A, Gabbiani C, Sorrentino F, Rigobello MP, Bindoli A, Geldbach TJ, Marrone A, Re N, Hartinger CG, Dyson PJ, Messori L. J. Med. Chem. 2008; 51:6773. [PubMed: 18834187]
38. Bindoli R, Rigobello MP, Scutari G, Gabbiani C, Casini A, Messori L. Coord. Chem. Rev. 2009; 253:1692.
39. Gabbiani C, Massai L, Scaletti F, Michelucci E, Maiore L, Cinellu MA, Messori L. J. Bio. Inorg. Chem. 2012; 17:1293. [PubMed: 23132507]
40. Uson R, Laguna A, Laguna M, Briggs D, Murray H, Fackler J. Inor. Synth. 1989; 26:85.
41. CrysAlisPro, Agilent Technologies, Version 1.171.35.19 (release 27-10-2011 CrysAlis171.NET) (compiled Oct 27 2011,15:02:11).
42. Altomare A, Burla MC, Camalli M, Cascarano GL, Giacovazzo C, Guagliardi A, Moliterni AGG, Polidori G, Spagna R. J. Appl. Cryst. 1999; 32:115.
43. Sheldrick GM. Acta Cryst. 2008; A64:112.
44. Nardelli MJ. Appl. Cryst. 1995; 28:659.
45. Farrugia LJJ. Appl. Cryst. 1997; 30:565.
46. Farrugia LJJ. Appl. Cryst. 2012; 45:849.

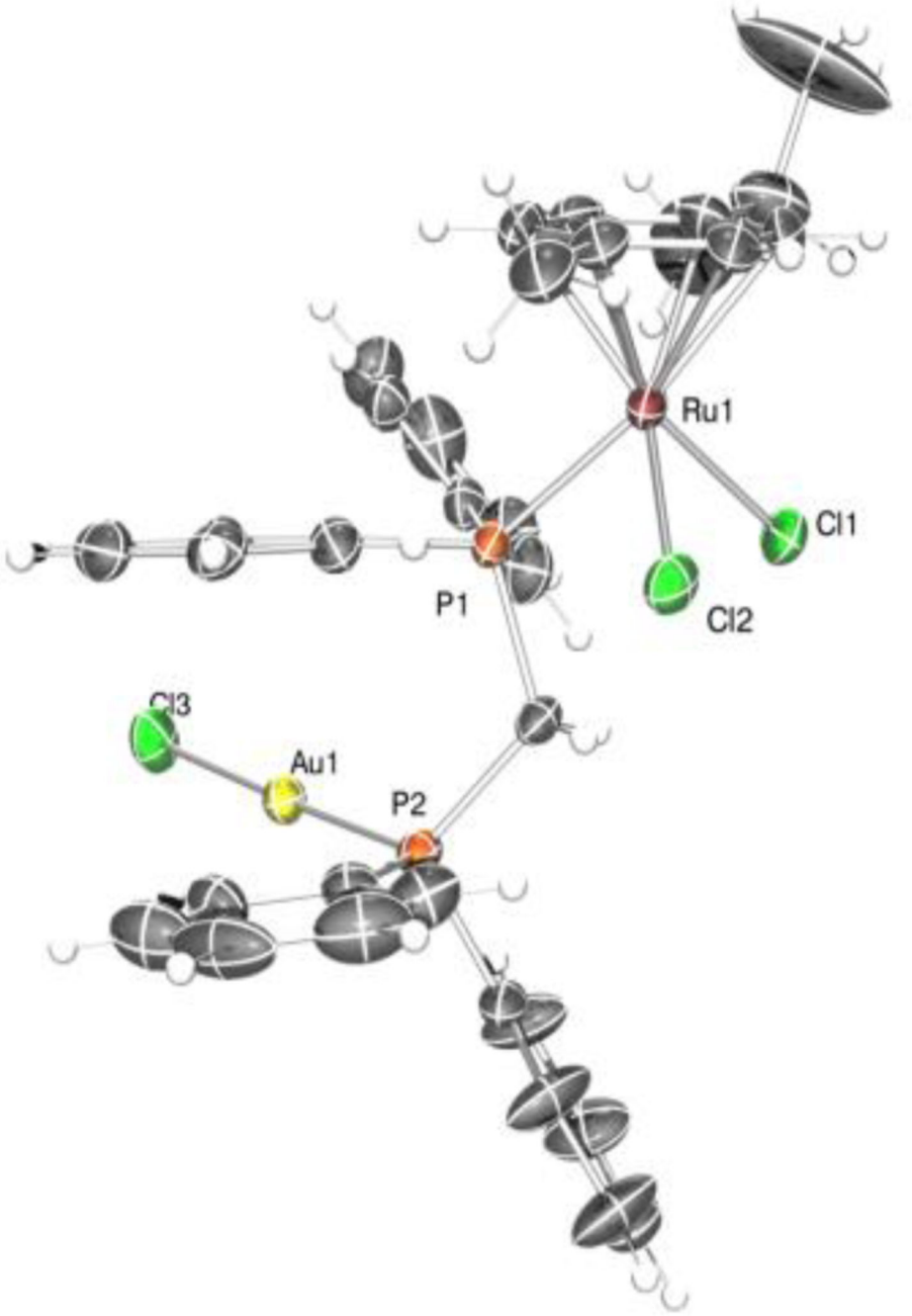

Figure 1.
ORTEP drawing of complex 1 with ellipsoids at 10% probability. Hydrogen atoms are not shown

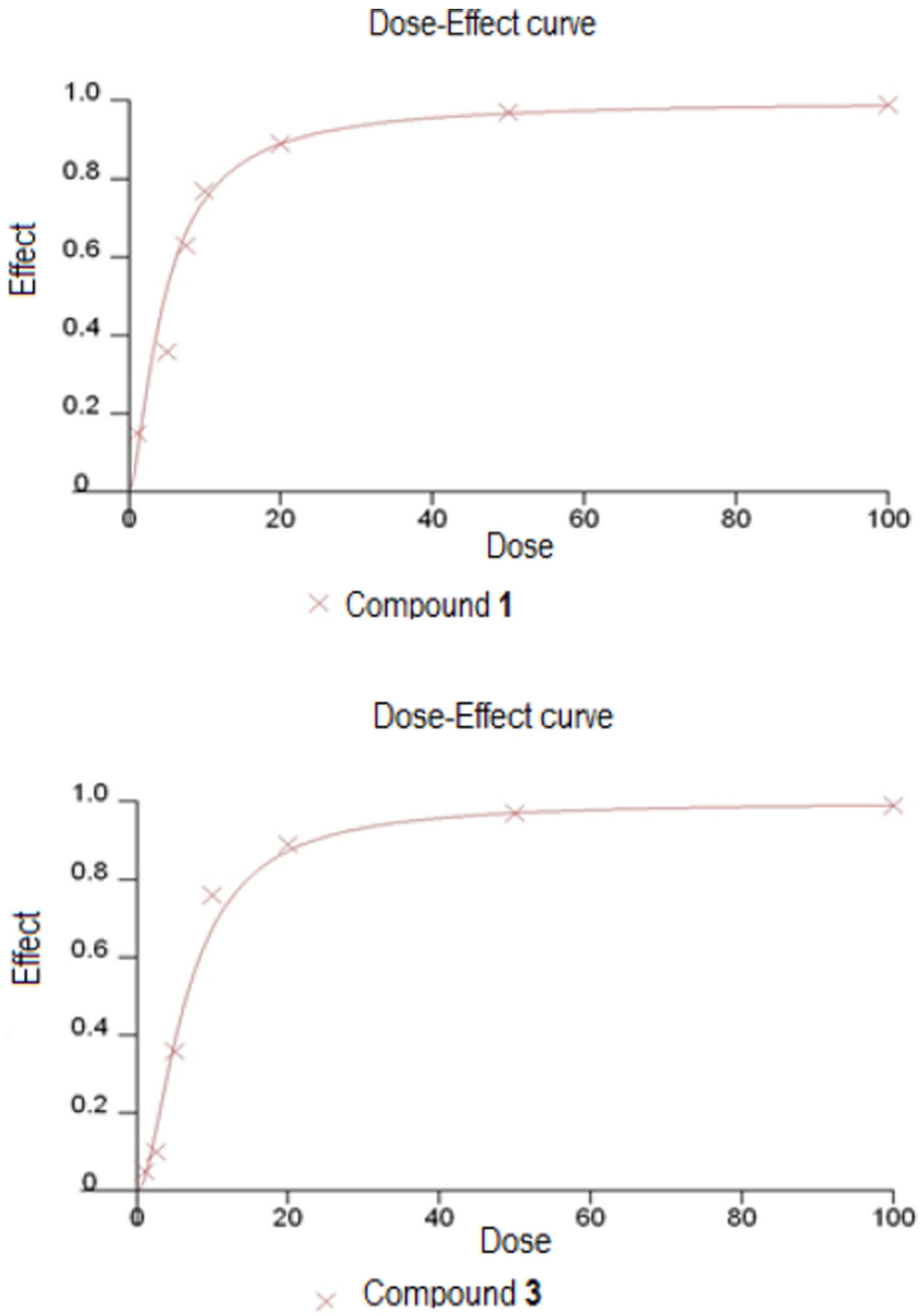

Figure 2.

Dose/Effect curve for compound **1** and **3** against HCT116 cells (after 48 h of incubation) calculated by fitting the data points with a sigmoidal curve using Calcusyn software

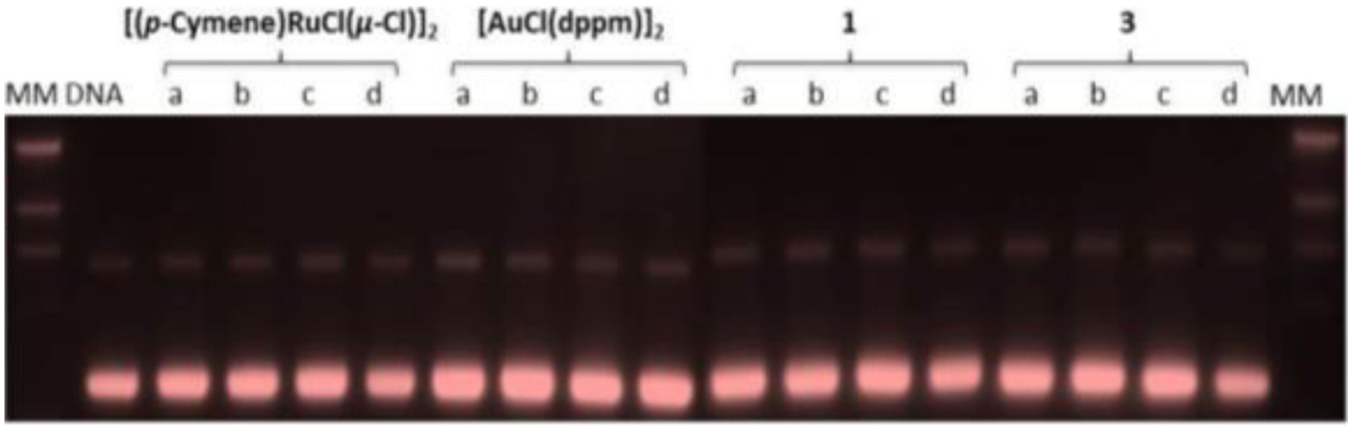

Figure 3.

Electrophoresis mobility shift assays for [Ru(p-cymene)Cl(μ-Cl)]$_2$, [AuCl(μ-dppm)]$_2$ and compounds **1** and **3** (see Experimental Section for details). DNA refers to untreated plasmid pBR322. Lanes a, b, c, and d correspond to metal/DNAbp ratios of 0.25, 0.5, 1.0, and 2.0, respectively

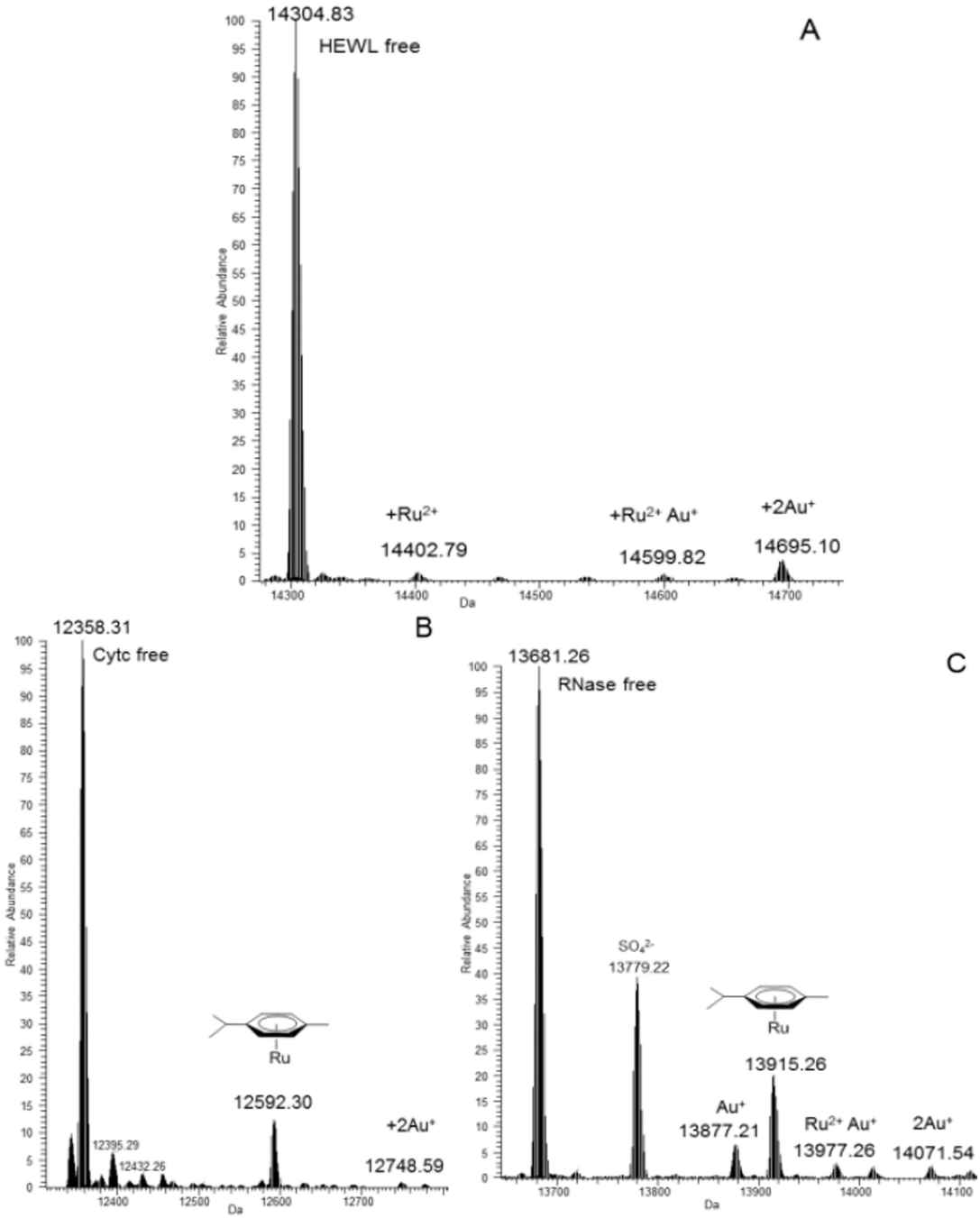

Figure 4.

A) Interaction between compound **1** and HEWL; B) Interaction between **3** and Cyt c; C) Interaction between **3** and RNase A. All of them 3:1 compound: protein molar ratio

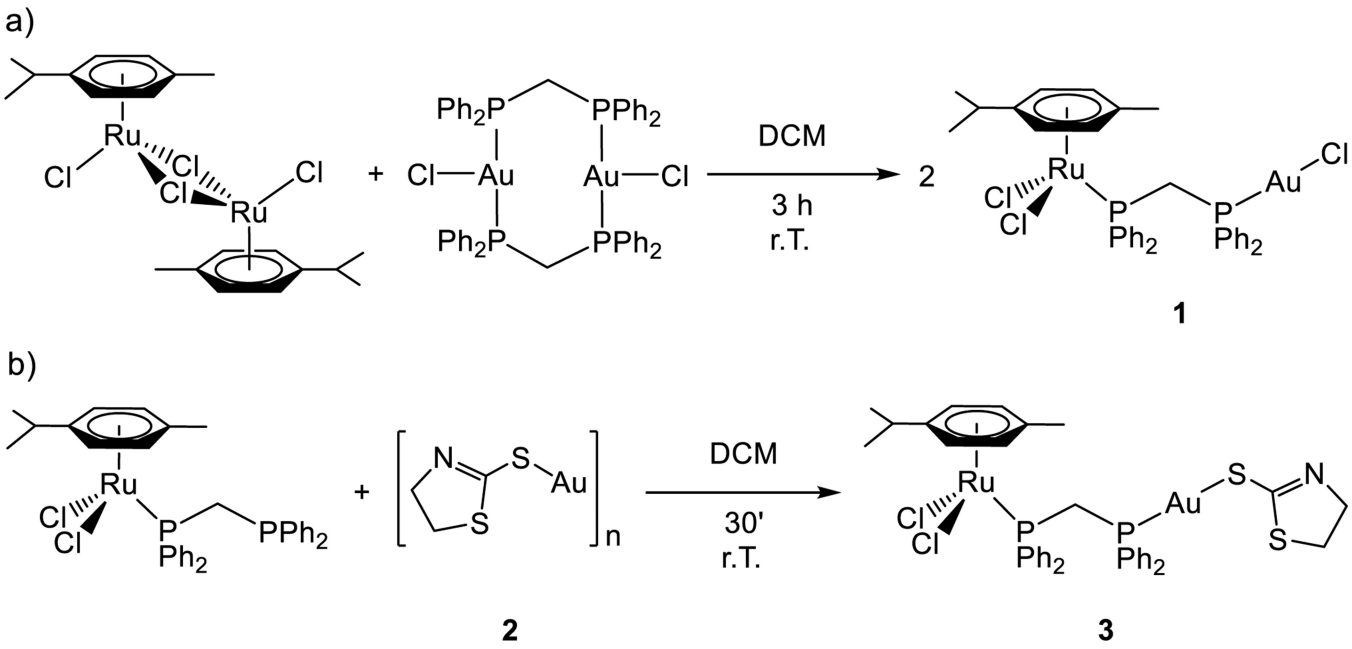

Scheme 1.

a) Synthesis of compound **1**; b) synthesis of compound **3**

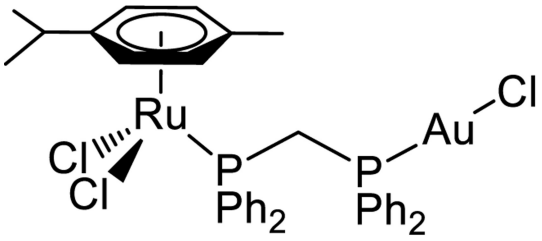

1

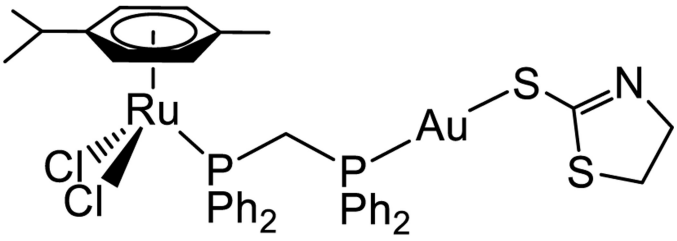

3

Chart 1.
[$RuCl_2$(*p*-cymene)(μ-dppm)AuCl] (**1**); [$RuCl_2$(*p*-cymene)(μ-dppm)Au(S-thiazoline)] (**3**).

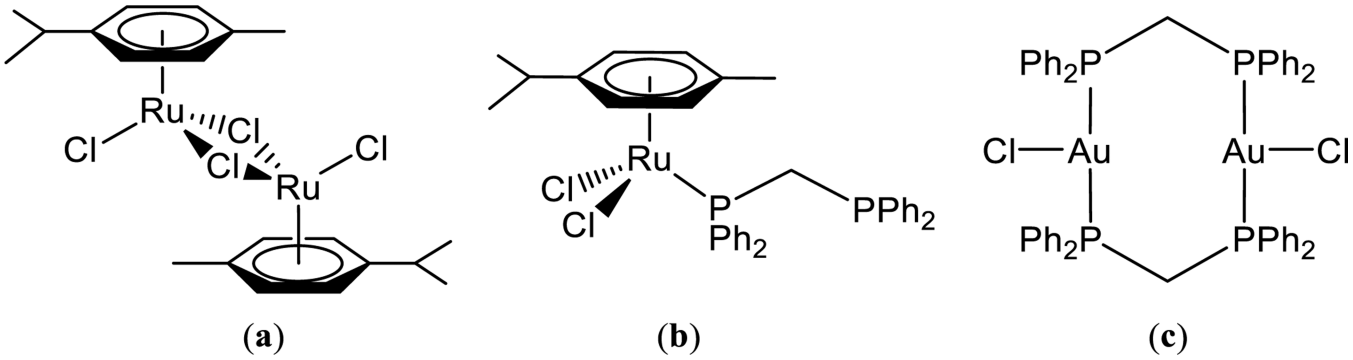

(**a**) (**b**) (**c**)

Chart 2.

Ru and Au reference compounds; (**a**) [Ru(*p*-cymene)Cl(μ-Cl)]$_2$[26](**b**) [Ru(*p*-cymene)Cl$_2$(*n*^{1}-dppm)]$_2$[28,29] (**c**)[(AuCl(μ-dppm)]$_2$[30]

Table 1

Selected Structural Parameters of complex 1 obtained from X-ray single crystal diffraction studies. Bond lengths in Å and angles in °.

Ru(1)-C(1)	2.2121(9)	Cl(1)-Ru(1)-Cl(2)	88.2(1)
Ru(1)-C(2)	2.1873(9)	Cl(1)-Ru(1)-P(1)	84.30(8)
Ru(1)-C(3)	2.172(1)	Cl(2)-Ru(1)-P(1)	87.29(8)
Ru(1)-C(4)	2.182(1)	P(2)-Au(1)-Cl(3)	177.88(9)
Ru(1)-C(5)	2.2067(9)	Ru(1)-P(1)-C(23)	110.3(3)
Ru(1)-C(6))	2.2217(9)	P(1)-C(23)-P(2)	119.1(5)
Ru(1)-Cl(1)	2.400(3)	C(23)-P(2)-Au(1)	113.0(3)
Ru(1)-Cl(2)	2.416(4)		
Ru(1)-P(1)	2.352(2)		
Au(1)-Cl(3)	2.275(4)		
Au(1)-P(2)	2.228(2)		

Table 2

In vitro IC50 (μM) of Tumor Cell Line by heterometallic complexes **1** and **3** and reference Ru and Au compounds. All compounds were dissolved in DMSO (1%) before addition to cell culture medium for a 48 h incubation period.

Compound	L929	HCT116		
	IC50	IC50	IC75	IC90
a (Ru)	243.4±9.9	73.7±2.2	313.3±7.1	1331.4±23.1
b (Ru)	39.6±2.1	21.9±1.7	228.7±2.3	2393.4±24.0
c (Au)	1.7±0.1	1.3±0.1	1.9±0.2	2.7±0.1
1	36.1±1.1	4.6±0.1	9.9±0.2	21.5±0.8
3	48.6±2.2	6.5±0.1	12.3±0.2	23.2±0.3

Table 3

Calculated tumour selectivity (IC50 L929/IC50HCT116) of tested complexes on cancer and normal cell cultures

a (Ru)	3.3
b (Ru)	1.8
c (Au)	1.3
1	7.8
3	7.5

Table 3

Inhibition of Capthesin B.[a]

Compound	IC50 (M)
1	3.14×10^{-5}
3	1.90×10^{-4}
b	1.43×10^{-4}

[a]Singlicate experiments.